ELSEVIER

Ecological Modelling 152 (2002) 47–64

ECOLOGICAL MODELLING

www.elsevier.com/locate/ecolmodel

The dynamics of a tri-trophic food chain with two-component populations from a biochemical perspective

P.P.F. Hanegraaf, B.W. Kooi *

Department of Theoretical Biology, Institute of Ecological Science, Faculty of Biology, Vrije Universiteit Amsterdam, De Boelelaan 1087, 1081 HV Amsterdam, The Netherlands

Received 15 March 2001; received in revised form 10 October 2001; accepted 18 October 2001

Abstract

Theoretical considerations and curve fitting of data support the proposition that models for heterotrophic organisms are more realistic when individuals consist of two components: reserves and structure. Predators that prey on a population of such individuals can choose to assimilate the reserves or the structure of the prey, or both. As a consequence, the Holling type II description we use for predator–prey interaction has to be revised. In this article we study tri-trophic food chains with two-component populations in a chemostat. The influence of different degrees of assimilation of reserves and structure on the long-term dynamics of the food chain is studied with bifurcation analysis of the governing system of ODEs. The results presented in bifurcation diagrams show large quantitative effects. The modelling will start at the individual level. The two components of the prey are assimilated in parallel and the usable portions are added to a common storage pool, the reserves. The energy stored in these reserve materials is used for maintenance and growth. The three processes, assimilation, maintenance and growth, are modelled as chemical reactions where mass and energy conservation laws are obeyed. With stationary solutions the growth rate has to be positive in order to compensate for predation and other causes of depletion. However, with oscillatory solutions, reversed growth can occur when time-periods exist where the reserves are less than needed to pay maintenance costs. When reversed growth is allowed, the two components can be transformed into each other without heat or product formation, which is unrealistic. This calls for a constraint on the maintenance requirements so that reversed growth does not occur. This constraint yields a new cause for extinction by nutrient enrichment for the two-component model.

Keywords: Bifurcation analysis; Continuous culture; Mass and energy balances; Food chain; Chemical reaction equation; Reversed growth

1. Introduction

In many ecological text books (Odum, 1996, p. 107), energy and material flow through the individual are described qualitatively as follows. The usable part of the food is assimilated and stored

* Corresponding author. Tel.: +31-20-444-7129; fax: +31-20-444-7123.

E-mail address: kooi@bio.vu.nl (B.W. Kooi).

0304-3800/02/$ - see front matter
PII: S0304-3800(01)00482-3

in reserve component, and the unusable part, the faeces, is ejected in the environment the individual lives in. A portion of the reserves is respired to provide maintenance energy to keep the body functioning and repaired. What is left is used for growth, that is the increase of structural component.

We will use the dynamic energy budget (DEB) model proposed in Kooijman (2000) to describe the dynamics of the individuals quantitatively. The individuals consist of two components, structure and reserve. In this approach the multitude of biochemical pathways that are present in individuals are lumped into three processes: assimilation, maintenance and growth. These processes are chemical reactions between the compounds of the individual and the compounds in its environment. Two-compartment models with a structural part and a storage part, are often used to describe nutrient-limited autotrophs (Droop, 1983; Lange and Oyarzun, 1992). We include reserves for the description of heterotrophs that have their main carbon- and energy-source as limiting nutrient. Food is not continuously available in natural environments, and reserves are needed to survive periods (which are relatively short with respect to the lifetime of the individuals) where nutrient is absent, if only to pay the cost of maintenance.

In this article we examine the behaviour of a tri-trophic food chain that consist of a nutrient, prey, predator and top-predator population, in a continuous culture (chemostat) environment. This means that predators can assimilate the reserves and the structure of their prey with different assimilation efficiencies.

We assume that all individuals that make up the population are identical. Then, assuming the Holling type II interaction between populations, the dynamics of the populations is obtained by superposition of the contributions of the individuals. In this way we obtain two ordinary differential equations for each trophic level of the food chain, except for the lowest level which is assumed to be an abiotic nutrient supplied to the chemostat reactor.

We consider modelling of biochemical detailed metabolic pathways broken down to the level of individual enzymatic reactions too complicated for the description of individuals and consequently for populations, communities and ecosystems. However, the representation of the transformations in a model in biochemical reactions of a restricted number of clustered pathways adds realism. This representation as biochemical reactions (Roels, 1983; Nielsen and Villadsen, 1994; Kooijman, 2000), explicitly assigns a number of properties to these state variables, such as the internal energy and the elemental and chemical composition. This allows analysis of ecosystems, that is communities including abiotic interactions with their environment, in keeping with the conservation laws for mass and energy and thermodynamic constraints. This allows for thermodynamics of an ecosystem without the need for quantities such as emergy and exergy, proposed in Nielsen and Ulanowicz (2000), Nielsen (2000), Jørgensen (2001).

In Hanegraaf et al. (2000), Hanegraaf and Muller (2001) we showed by curve fitting experimental data, that our two-component model can describe the dynamics of the varying macromolecular composition of microorganisms. Moreover, the addition of elemental and enthalpy balances obtained with the chemical reaction equations allows the description of product formation, nutrient consumption and heat formation (Hanegraaf, 1997; Kooijman et al., 1999; Hanegraaf et al., 2000; Kooijman, 2000; Kooi and Hanegraaf, 2001). This approach enables the application of the population model developed here in an ecosystem model, where physical interactions with the environment are taken into account (see DeAngelis, 1992; Polis and Winemiller, 1996; Loladze et al., 2001).

In earlier work, the equations for product formation were obtained as a byproduct of the mathematical proof that the solution of the system of state equations is bounded (Kooi et al., 1998, 1999). Later we showed that these equations for product formation are a special case of the product equations one obtains from the chemical reaction equations (Kooi and Hanegraaf, 2001). In this special case the composition of reserves and structure must be equal. More-

over, reserves and structure can be transformed into each other without heat or product formation, and this is unrealistic.

The special case is consistent with the model choice that structure can be used for maintenance purposes in case the reserve density is not sufficient to pay these costs. When structure is used for maintenance it will shrink (reversed growth). In this article we examine the consequences of reversed growth for the long-term dynamics of a tri-trophic food chain in a chemostat. As we shall see, similar to the bi-trophic food chain case described in Kooi and Hanegraaf (2001), with the tri-trophic food chain a major area of non-stationary coexistence in the bifurcation diagram is strongly affected by the model choice that reversed growth is not allowed and we find new causes for extinction by nutrient enrichment.

Building on earlier work (Kooi et al., 1998, 1999; Kooijman et al., 1999; Hanegraaf et al., 2000; Kooi and Hanegraaf, 2001), we will construct bifurcation diagrams which summarize the long-term dynamic behaviour of the model system depending on parameter values. Regions of a bifurcation diagram mark different qualitative dynamic behaviour, such as the presence or absence of a predator. The behaviour of the tri-trophic food chain can be complex, even though we use a biochemically simple model in a simple continuous feed environment.

Variation of the parameter that describes the nutritional value of both components gives the influence of different degrees of assimilation of reserves and structure on the long-term dynamics of the food chain under various environmental conditions.

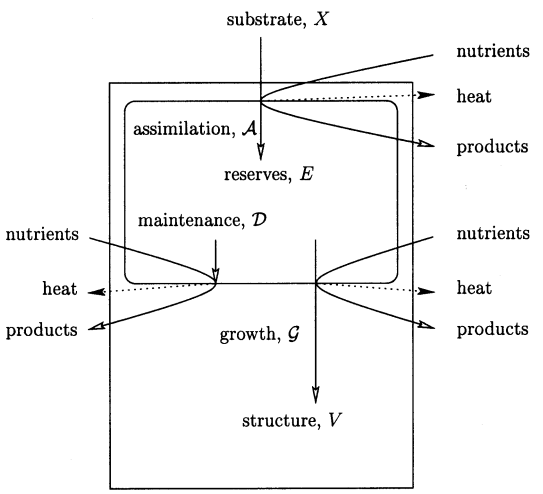

Fig. 1. Fluxes in an individual. The individual (indicated by the large square) consists of two components: structure and reserves. There are three processes: nutrient is transformed into reserves by assimilation, reserves are used for maintenance of structure, and reserves are used for growth (i.e. increase of structure). Products and heat are produced and non-limiting nutrients are consumed in each process.

2. Fluxes in individuals

Even for simple models, it is important to state explicitly the dynamics of all compounds, including the non-reproducing nutrients, non-limiting nutrients and products. Therefore, we begin with mass and energy balances in this section, where each independent process is represented as a chemical reaction equation. Conditions for the conservation of mass (elements) and energy are derived for each independent process.

The fluxes in an individual organism are outlined in Fig. 1. The net result of uptake and assimilation, maintenance and growth, can be written as a macroscopic chemical reaction equation. For example,

$$J_X \overset{\text{nutrient, } X}{C_1 H_{n_{HX}} O_{n_{OX}} N_{n_{NX}}} + \overset{\text{ammonia, } N}{J_N H_3 N_1} + \overset{\text{oxygen, } O}{J_O O_2} \rightarrow J_E \overset{\text{reserves, } E}{C_1 H_{n_{HE}} O_{n_{OE}} N_{n_{NE}}} + J_V \overset{\text{structural mass, } V}{C_1 H_{n_{HV}} O_{n_{OV}} N_{n_{NV}}} + \overset{\text{carbon dioxide, } C}{J_C C_1 O_2} + \overset{\text{water, } H}{J_H H_2 O_1} + J_P \overset{\text{product, } P}{C_1 H_{n_{HP}} O_{n_{OP}} N_{n_{NP}}} \quad (1)$$

where n_{ec} is the chemical index or the number of element $e \in \{C, H O, N, \ldots\}$ in compound, $c \in \{C, H, O, N, \ldots\}$.

All compounds are measured in C-moles. The biomass of the compounds constituting the individual is denoted by M_c, $c \in \{V, E\}$, that is the structural component V and the storage compo-

nent E. The rate of change of these compounds is denoted by $J_c = \mathrm{d}M_c/\mathrm{d}t,\ c \in \{V, E\}$. When the individual grows (that is, increases its structural biomass) we have $J_V > 0$ and when it shrinks $J_V < 0$. When the individual extracts per unit of time more material from the storage pool than it supplies into it, we have $J_E < 0$. The flux of a compound which is ingested from or excreted into the environment by the individual is denoted by $J_c,\ c \in \{X, O, N, C, H, P\}$ as a result of net utilization ($J_c < 0,\ c \in \{X, O, N\}$) or production ($J_c > 0,\ c \in \{C, H, P\}$). Thus the compounds at the top row of Eq. (1) are ingested, the compounds at the second row constitute the individual and those at the bottom row are excreted. Nutrient X forms the carbon- and energy-source of the individual and products P, such as faeces, are produced. We conclude that we have in Eq. (1) always $J_X > 0$ and $J_P > 0$, but in general the other fluxes can be positive or negative. Compounds $c \notin \{X, V, E, P\}$ are organic or inorganic products and non-limiting nutrients. In general many other products and nutrients than indicated in Eq. (1) can be present.

We continue with the case that a predator consumes prey. Then the reserves and structure of the prey serve as nutrient for the predator. The prey components are part of individual prey, and are taken up simultaneously by the predator. So, effectively we have two carbon- and energy-sources, XV and XE. The fluxes of XV and XE are related as will be derived below.

The law of conservation of mass holds for the elemental balances

$$\mathbf{n}_{\mathrm{e}c}\mathbf{J}_c = 0, \tag{2a}$$

$$\mathbf{n}_{\mathrm{e}c} \overset{\mathrm{def}}{=} \begin{pmatrix} 1 & 1 & 1 & 1 & 1 & 0 & 0 & 0 & \cdots \\ n_{\mathrm{H}XV} & n_{\mathrm{H}XE} & n_{\mathrm{H}V} & n_{\mathrm{H}E} & n_{\mathrm{H}C} & n_{\mathrm{H}H} & n_{\mathrm{H}O} & n_{\mathrm{H}N} & \cdots \\ n_{\mathrm{O}XV} & n_{\mathrm{O}XE} & n_{\mathrm{O}V} & n_{\mathrm{O}E} & n_{\mathrm{O}C} & n_{\mathrm{O}H} & n_{\mathrm{O}O} & n_{\mathrm{O}N} & \cdots \\ n_{\mathrm{N}XV} & n_{\mathrm{N}XE} & n_{\mathrm{N}V} & n_{\mathrm{N}E} & n_{\mathrm{N}C} & n_{\mathrm{N}H} & n_{\mathrm{N}O} & n_{\mathrm{N}N} & \cdots \\ \vdots & \vdots & \vdots & \vdots & \vdots & \vdots & \vdots & \vdots & \ddots \end{pmatrix}, \tag{2b}$$

$$\mathbf{J}_c^T \overset{\mathrm{def}}{=} (J_{XV} \quad J_{XE} \quad J_V \quad J_E \quad J_C \quad J_H \quad J_O \quad J_N \quad \cdots). \tag{2c}$$

All elements of the elemental composition matrix $\mathbf{n}_{\mathrm{e}c}$ are positive for both 'reactants' with negative fluxes, $J_c < 0$, and 'products' with positive fluxes, $J_c > 0$. For the number of carbon in compound c we have that $n_{\mathrm{C}c},\ c \in \{C, H, O, N, \ldots\}$ equals 0 or 1. For example the compound carbon dioxide CO_2 has $n_{CC} = 1$ and water H_2O has $n_{CH} = 0$. In principle, all elements present in the individual are taken into account.

As the chemical reactions occur in the open system (exchange of matter with the environment is possible) under isobaric circumstances, heat may be evolved or absorbed. Generally heat is generated, associated with a change in enthalpy which acts as a 'potential for heat flux' at constant pressure (Kondepudi and Prigogine, 1998). It is assumed that the temperature of the system is kept constant. The law of conservation of energy holds for the enthalpy balance

$$\tilde{\mathbf{h}}_c^T\mathbf{J}_c + p_H = 0, \tag{3a}$$

$$\tilde{\mathbf{h}}_c^T \overset{\mathrm{def}}{=} (\tilde{h}_{XV} \quad \tilde{h}_{XE} \quad \tilde{h}_V \quad \tilde{h}_E \quad \tilde{h}_C \quad \tilde{h}_H \quad \tilde{h}_O \quad \tilde{h}_N \quad \cdots), \tag{3b}$$

where $\tilde{h}_c$ is the C-molar enthalpy density of compound $c \in \{C, H, O, N, \ldots\}$ and p_H is the rate of heat formation.

The basic energy fluxes for assimilation are denoted by $p_{\mathscr{A}\mathscr{V}}$ and $p_{\mathscr{A}\mathscr{E}}$, for maintenance by $p_{\mathscr{D}}$ and for growth by $p_{\mathscr{G}}$. The mass fluxes are related to these basic energy fluxes as,

$$\mathbf{J}_c = \boldsymbol{\eta}_{cL}\mathbf{p}_p, \tag{4a}$$

where

$$\boldsymbol{\eta}_{c\mathscr{P}} \overset{\text{def}}{=} \begin{pmatrix} h^{-1}_{\mathscr{AV}XV} & h^{-1}_{\mathscr{AE}XV} & h^{-1}_{\mathscr{D}XV} & h^{-1}_{\mathscr{G}XV} \\ h^{-1}_{\mathscr{AV}XE} & h^{-1}_{\mathscr{AE}XE} & h^{-1}_{\mathscr{D}XE} & h^{-1}_{\mathscr{G}XE} \\ h^{-1}_{\mathscr{AV}V} & h^{-1}_{\mathscr{AE}V} & h^{-1}_{\mathscr{D}V} & h^{-1}_{\mathscr{G}V} \\ h^{-1}_{\mathscr{AV}E} & h^{-1}_{\mathscr{AE}E} & h^{-1}_{\mathscr{D}E} & h^{-1}_{\mathscr{G}E} \\ h^{-1}_{\mathscr{AV}C} & h^{-1}_{\mathscr{AE}C} & h^{-1}_{\mathscr{D}C} & h^{-1}_{\mathscr{G}C} \\ \vdots & \vdots & \vdots & \vdots \end{pmatrix} = \begin{pmatrix} h^{-1}_{\mathscr{AV}XV} & 0 & 0 & 0 \\ 0 & h^{-1}_{\mathscr{AE}XE} & 0 & 0 \\ 0 & 0 & 0 & h^{-1}_{\mathscr{G}V} \\ \tilde{h}^{-1}_{E} & \tilde{h}^{-1}_{E} & -\tilde{h}^{-1}_{E} & -\tilde{h}^{-1}_{E} \\ h^{-1}_{\mathscr{AV}C} & h^{-1}_{\mathscr{AE}C} & h^{-1}_{\mathscr{D}C} & h^{-1}_{\mathscr{G}C} \\ \vdots & \vdots & \vdots & \vdots \end{pmatrix}, \tag{4b}$$

$$\mathbf{p}^{T}_{\mathscr{P}} \overset{\text{def}}{=} (\mathbf{p}_{\mathscr{AV}} \quad \mathbf{p}_{\mathscr{AE}} \quad \mathbf{p}_{\mathscr{D}} \quad \mathbf{p}_{\mathscr{G}}), \tag{4c}$$

where $h_{\mathscr{P}c}$ denotes the energy flux per flux of mass for process $\mathscr{P}\in\{\mathscr{AV}, \mathscr{AE}, \mathscr{D}, \mathscr{G}\}$ and chemical compound $c\in\{\text{XV, XE, } V, E, C, \ldots\}$. Elements $h_{\mathscr{P}c}$ of the stoichiometric matrix $\boldsymbol{\eta}_{c\mathscr{P}}$ are conversion coefficients and serve as model parameters that couple energy and mass fluxes.

Reserves are utilized for maintenance and growth while assimilation contributes to reserve formation. Hence the enthalpy balance for the reserves reads,

$$\tilde{h}_E J_E = (p_{\mathscr{AV}} + p_{\mathscr{AE}} - p_{\mathscr{D}} - p_{\mathscr{G}}). \tag{5}$$

So, in the fourth row of Eq. (4b), $h_{\mathscr{AV}E}$ and $h_{\mathscr{AE}E}$ equal the C-molar enthalpy density of the reserves $\tilde{h}_E$, while the $h_{\mathscr{D}E}$ and $h_{\mathscr{G}E}$ equal $-\tilde{h}_E$. We remark that the overhead costs for the assimilation processes is not included in assimilation fluxes $p_{\mathscr{AV}} + p_{\mathscr{AE}}$, while the overhead costs for the growth process are included in the growth flux $p_{\mathscr{G}}$.

The rate of heat production in Eq. (3) is related to the basic energy fluxes as,

$$p_T = \eta_{T\mathscr{P}} \mathrm{p}_{\mathscr{P}}, \tag{6a}$$

$$\boldsymbol{\eta}_{T\mathscr{P}} \overset{\text{def}}{=} (h^{-1}_{\mathscr{AV}T} \quad h^{-1}_{\mathscr{AE}T} \quad h^{-1}_{\mathscr{D}T} \quad h^{-1}_{\mathscr{G}T}). \tag{6b}$$

Microscopic chemical reaction equations and elemental balances, analogous to Eq. (1), can be constructed for each independent process $p_{\mathscr{AV}}, p_{\mathscr{AE}}, p_{\mathscr{D}}$ and $p_{\mathscr{G}}$ (Hanegraaf, 1997). With independent processes we mean that their process rates taken as functions of time over an arbitrary time interval, are linear independent. This means that these processes are not regulated by a single biological control mechanism. For macroscopic chemical reaction Eq. (1), the microscopic chemical reaction equation for the growth process reads

$$h^{-1}_{\mathscr{G}E}\mathrm{C}_1\mathrm{H}_{n_{\mathrm{H}E}}\mathrm{O}_{n_{\mathrm{O}E}}\mathrm{N}_{n_{\mathrm{N}E}} + \overset{\text{reserves, } E}{} + h^{-1}_{\mathscr{G}N}\overset{\text{ammonia, } N}{\mathrm{H}_3\mathrm{N}_1} + h^{-1}_{\mathscr{G}O}\overset{\text{oxygen, } O}{\mathrm{O}_2}$$
$$\rightarrow h^{-1}_{\mathscr{G}V}\overset{\text{structural mass, } V}{\mathrm{C}_1\mathrm{H}_{n_{\mathrm{H}V}}\mathrm{O}_{n_{\mathrm{O}V}}\mathrm{N}_{n_{\mathrm{N}V}}} + h^{-1}_{\mathscr{G}C}\overset{\text{carbon dioxide, } C}{\mathrm{C}_1\mathrm{O}_2}$$
$$+ h^{-1}_{\mathscr{G}A}\overset{\text{water, } H}{\mathrm{H}_2\mathrm{O}_1} + h^{-1}_{\mathscr{G}P}\mathrm{C}_1\overset{\text{product, } P}{\mathrm{H}_{n_{\mathrm{H}P}}\mathrm{O}_{n_{\mathrm{O}P}}\mathrm{N}_{n_{\mathrm{N}P}}}, \tag{7}$$

where we used the stoichiometry from Eq. (4b).

The flux of element e is a linear combination of fluxes $p_{\mathscr{AV}}, p_{\mathscr{AE}}, p_{\mathscr{D}}$ and $p_{\mathscr{G}}$.

$$\mathbf{n}_{\mathrm{e}c}\mathbf{J}_c = \mathbf{n}_{\mathrm{e}c}\boldsymbol{\eta}_{c\mathscr{P}}\mathbf{p}_{\mathscr{P}} = 0. \tag{8}$$

As the processes $\mathscr{P}\in\{\mathscr{AV}, \mathscr{AE}, \mathscr{D}, \mathscr{G}\}$ are independent, this expression must hold for any $\mathbf{p}_{\mathscr{P}}$ and therefore $\mathbf{n}_{\mathrm{e}c}\boldsymbol{\eta}_{c\mathscr{P}} = 0$. As a consequence, there are four conditions per element. For instance, the condition related to growth is,

$$\frac{n_{\mathrm{e}V}}{h_{\mathscr{G}V}} - \frac{n_{\mathrm{e}E}}{\tilde{h}_E} + \sum_{c\in\{C,\,H,\,O,\,N,\,\ldots\}} \frac{n_{\mathrm{e}c}}{h_{\mathscr{G}c}} = 0. \tag{9}$$

The sum of the enthalpy fluxes and the heat rate can also be written as a linear combination of energy fluxes associated with the basic processes, $p_{\mathscr{AV}}, p_{\mathscr{AE}}, p_{\mathscr{D}}$ and $p_{\mathscr{G}}$, with Eqs. (3a) and (6a),

$$\tilde{\mathbf{h}}^{T}_c\mathbf{J}_c + p_T = \tilde{\mathbf{h}}^{T}_c\boldsymbol{\eta}_{c\mathscr{P}}\mathbf{p}_{\mathscr{P}} + \boldsymbol{\eta}_{T\mathscr{P}}\mathbf{p}_{\mathscr{P}} = 0. \tag{10}$$

As for the mass fluxes, the processes $\mathscr{P}\in\{\mathscr{AV}, \mathscr{AE}, \mathscr{D}, \mathscr{G}\}$ are independent, and we have $\tilde{\mathbf{h}}^{T}_c\boldsymbol{\eta}_{c\mathscr{P}} + \boldsymbol{\eta}_{T\mathscr{P}}$ is zero. This gives one condition per process, for example for the growth process $\mathscr{G}$,

$$\frac{\tilde{h}_V}{h_{\mathscr{G}V}} - 1 + \sum_{c\in\{C,\,H,\,O,\,N,\,\ldots\}} \frac{\tilde{h}_c}{h_{\mathscr{G}c}} + \frac{1}{h_{\mathscr{G}T}} = 0. \tag{11}$$

Eqs. (9) and (11) show how macroscopic fluxes $\mathbf{J}_c$ (Eq. (2c)) and $\tilde{\mathbf{h}}_c$ (Eq. (3b)) are related to microscopic biochemical stoichiometric coefficients (Eq. (4b)).

The next section is about the population level where we will couple the basic energy fluxes (Eq. (6a)) for the three processes to the two state

variables, the mass of the structural component, M_V, and the mass of the storage component, M_E. At the population level the interaction between individuals of a predator species and the individuals of the prey species is formulated. In the description of fluxes related to the assimilation processes it must be taken into account that prey and predator consist of two components.

3. Fluxes in populations

We assume that all individuals belonging to a population are identical. The structural biomass of a population is just the biomass of each individual times the number of individuals. A similar relationship holds for the reserves. Each population consists of all its individuals in the culture volume of the reactor, V_C, and we will define densities with respect to this volume. For the structural biomass density, denoted by x_i, and the reserves mass density, z_i, we have

$$x_i = M_{Vi} = \frac{1}{V_C}\sum_l M_{Vil}, \quad z_i = M_{Ei} = \frac{1}{V_C}\sum_l M_{Eil}. \tag{12a}$$

In the DEB model the reserves mass density itself is not used as a state variable but the scaled energy density, denoted by e_i, defined by

$$e_i = \frac{\sum_l M_{Eil}}{\sum_l M_{Vil}[M_{Emi}]} = \frac{z_i}{x_i[M_{Emi}]}, \tag{12b}$$

where l labels the individuals. The parameter $[M_{Emi}]$ is the maximum reserve biomass density which is a species dependent parameter so that $0 \le e_i \le 1$.

All mass density fluxes are given by $J_{ci} = \Sigma_l J_{cil}/V_C$ with $c \in \{X, A, D, G\}$, and the energy density fluxes $p_{\mathscr{P}i} = \Sigma_l p_{\mathscr{P}il}/V_C$ with process-index $\mathscr{P} \in \{\mathscr{A}, \mathscr{D}, \mathscr{G}\}$. Because mass and energy fluxes are additive over all individuals the constitutive relationships Eq. (4a) hold also for these density fluxes J_{ci} and $p_{\mathscr{P}i}$ at the population level.

We will assume that the interaction between the different trophic levels is described by a Holling type II functional response defined by,

$$f_{i-1,i}(x_{i-1}) = \frac{x_{i-1}}{k_{i-1,i} + x_{i-1}}, \tag{13}$$

where $k_{i-1,i}$ is the saturation constant. This needs explanation since the prey can consist of two components and here the functional response depends only the structural component and not on the reserve component. We assume that the assimilation rate of the (more temporary) storage materials is much faster than for the (more permanent) structural component. Thus, the handling time is completely determined by that for the structural component which is same for each individual in the population by assumption while the search time is not affected by the reserve component either.

The energy fluxes compatible with the DEB model read

$$\begin{pmatrix} \mathbf{p}_{\mathscr{A}\mathscr{V}i} \\ \mathbf{p}_{\mathscr{A}\mathscr{E}i} \\ \mathbf{p}_{\mathscr{D}i} \\ \mathbf{p}_{\mathscr{G}i} \end{pmatrix} = \begin{pmatrix} \mathbf{I}_{i-1,i}\, \mathbf{f}_{i-1,i}(\mathbf{x}_{i-1})\mathbf{h}_{\mathscr{A}\mathscr{V}XVi} \\ \mathbf{I}_{i-1,i}\, \mathbf{f}_{i-1,i}(\mathbf{x}_{i-1})\mathbf{e}_{i-1}[\mathbf{M}_{Em(i-1)}]\mathbf{h}_{\mathscr{A}\mathscr{E}XEi} \\ \mathbf{m}_i \mathbf{h}_{\mathscr{G}Vi} \\ \dfrac{v_{i-1,i}e_i - m_i g_i}{e_i + g_i}\, \mathbf{h}_{\mathscr{G}Vi} \end{pmatrix} x_i. \tag{14}$$

For the assimilation energy flux $p_{\mathscr{A}i}$ there is input from the two components, thus

$$\mathbf{p}_{\mathscr{A}i} = \mathbf{p}_{\mathscr{A}\mathscr{V}i} + \mathbf{p}_{\mathscr{A}\mathscr{E}i} = \left(1 + \frac{_{i-1,i}\mathbf{e}_{i-1}}{\mathbf{g}_{i-1}}\right) \mathbf{I}_{i-1,i}\, \mathbf{f}_{i-1,i}(\mathbf{x}_{i-1})\mathbf{x}_i h_{\mathscr{A}\mathscr{V}XVi}, \tag{15}$$

where $v_{i-1,i}$ and g_i are defined by,

$$_{i-1,i} = \frac{\mathbf{I}_{i-1,i}\left(1 + \dfrac{\rho_{i-1,i}}{g_{i-1}}\right)\mathbf{h}_{\mathscr{A}\mathscr{V}XVi}}{\tilde{\mathbf{h}}_{Ei}[\mathbf{M}_{Emi}]}; \qquad \mathbf{g}_i = \frac{1}{_i[\mathbf{M}_{Emi}]}. \tag{16}$$

The parameter g_i is proportional to the energetic costs for growth, that is the amount of energy liberated from the reserves for growth and $\gamma_i g_i$ is the part actually used for the growth process. The

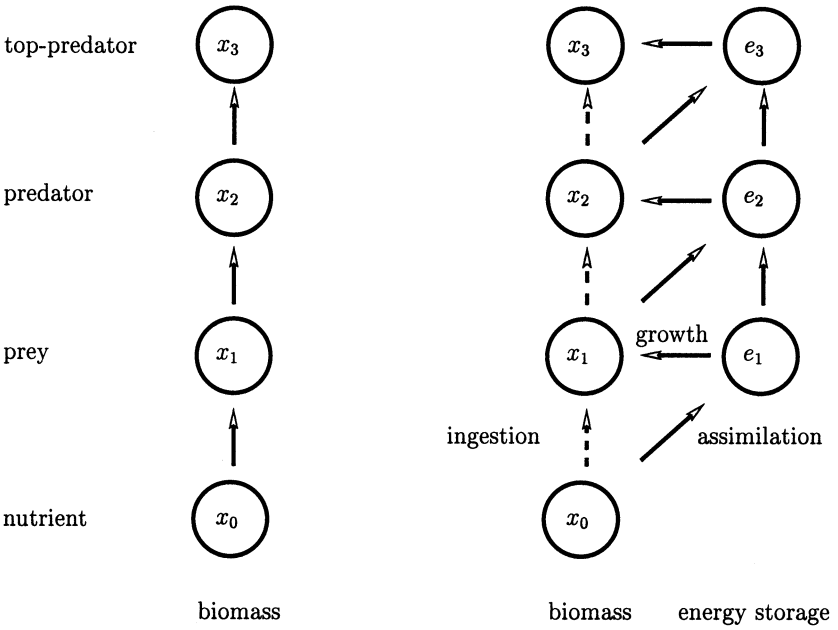

Fig. 2. Trophic interactions between the different trophic levels of a food chain for one-component (left) and two-component model (right). In the two-component model ingestion rate depends on structural biomass, assimilation rate depends on both structural and reserve biomass and growth rate on reserve biomass.

parameter $\rho_{i-1,i}$ is the ratio of nutritional value of prey components, a dimensionless constant

$$_i = \frac{\tilde{\mathbf{h}}_{Ei}}{\mathbf{h}_{\mathscr{G}Vi}}, \quad _{i-1,i} = \frac{\mathbf{h}_{\mathscr{A}\mathscr{E}XEi}}{_{i-1}\mathbf{h}_{\mathscr{A}\mathscr{V}XVi}}. \tag{17}$$

The expressions of the changes of the biomass of the structure and reserves at the population level J_{E1} and J_{V1}, Eq. (4a) can be used with Eq. (14) to derive the state equations for the dynamics of the scaled reserve mass and structural biomass of the population.

$$\frac{\mathrm{d}e_i}{\mathrm{d}t} = v_{i-1,i}\left(\frac{g_{i-1}+\rho_{i-1,i}e_{i-1}}{g_{i-1}+\rho_{i-1,i}} f_{i-1,i}(x_{i-1}) - e_i\right), \tag{18a}$$

$$\frac{\mathrm{d}x_i}{\mathrm{d}t} = \left(\frac{v_{i-1,i}e_i - m_i g_i}{e_i + g_i}\right)x_i. \tag{18b}$$

The expression for the sum of the mass fluxes belonging to the products, J_{ci}, $c \in \{C, H, O, N, \ldots\}$, is

$$\sum_{c\in\{C,H,O,N,\ldots\}} J_{ci} = \left(\left(1+\frac{e_{i-1}}{\gamma_{i-1}g_{i-1}}\right)I_{i-1,i} - \frac{v_{i-1,i}}{\gamma_i g_i}\frac{g_{i-1}+\rho_{i-1,i}e_{i-1}}{g_{i-1}+\rho_{i-1,i}}\right) f_{i-1,i}x_i + \left(\frac{m_i}{\gamma_i} + \left(\frac{1}{\gamma_i}-1\right)\left(\frac{v_{i-1,i}e_i - m_i g_i}{e_i+g_i}\right)\right)x_i, \tag{19}$$

where $v_{i-1,i}$ and g_i are given in Eq. (16) and $\rho_{i-1,i}$ and γ_{i-1} in Eq. (17). Notice that the prey population described by the state variables x_1 and e_1 takes up the nutrient x_0 only, so $e_0 = 0$ and $\gamma_0 = 1$.

4. The tri-trophic food chain in the chemostat

The chemostat is a well stirred reactor to which medium is added from a reservoir at time-invariant rate D, the dilution rate. As culture, composed of the community of the populations together with nutrients and products, is removed from the reactor at the same rate, the culture volume V_C remains constant.

One limiting carbon and energy source, with reservoir density x_r, is supplied to the chemostat reactor. Let $x_0(t)$ denote the density of this nutrient in the culture and we recall that $x_i(t)$, $i=1, 2, 3$ denote the structural biomass densities of prey, predator and top-predator and $e_i(t)$ for $i=1, 2, 3$ denote the scaled reserve densities for the three trophic levels, see Fig. 2. The state equations for a tri-trophic food chain reads

Table 1
Parameters and state variables

Parameter	Dimension	Interpretation
D	t^{-1}	Dilution rate
e_i	–	Reserve biomass density
g_i	–	Energy investment ratio, $\propto$ costs for growth
$\tilde{h}_{ci}$	e m^{-1}	C-molar enthalpy density of compound c
$h_{\mathscr{P}ci}$	e m^{-1} t^{-1}	Energy flux for process $\mathscr{P}$ per flux of mass of compound c
$I_{i-1,i}$	m m^{-1} t^{-1}	Maximum food uptake rate
J_{ci}	m V^{-1} t^{-1}	Mass flux density
$k_{i-1,i}$	m V^{-1}	Saturation constant
m_i	t^{-1}	Maintenance rate coefficient
M_{ci}	m V^{-1}	Biomass density
$[M_{Emi}]$	m m^{-1}	Maximum mass reserves per structural mass
$p_{\mathscr{P}i}$	e V^{-1} t^{-1}	Energy flux
q_i	m V^{-1}	Product mass density
t	t	Time
x_0	m V^{-1}	Nutrient density
x_i	m V^{-1}	Structural biomass density
x_r	m V^{-1}	Nutrient concentration in reservoir
$y_{i-1,i}$	m m^{-1}	Maximum yield
z_i	m V^{-1}	Reserve biomass density
$\eta_{c\mathscr{P}i}$	m e^{-1}	Flux mass for compound c per flux energy of process $\mathscr{P}$
$\eta_{T\mathscr{P}i}$	m e^{-1}	Flux energy of waste-heat per flux energy of process $\mathscr{P}$
$\mu_{i-1,i}$	t^{-1}	Maximum population growth rate
γ_I	–	Efficiency of growth process
$\rho_{i-1,i}$	–	Ratio of nutritional values for structure and reserves
$v_{i-1,i}$	t^{-1}	Energy conductance, $\propto$ assimilation rate

t, time; m, biomass; e, energy; V, volume of the reactor. The index i denotes the trophic level, $\mathscr{P}\in\{\mathscr{A}, \mathscr{D}, \mathscr{G}\}$ a process and $c\in\{X, V, E, A, D, G\}$ a chemical compound.

$$\frac{dx_0}{dt} = (x_r - x_0)D - I_{0,1}x_1 f_{0,1}(x_0), \tag{20a}$$

$$\frac{de_1}{dt} = v_{0,1}(f_{0,1}(x_0) - e_1), \tag{20b}$$

$$\frac{dx_1}{dt} = \left(\frac{v_{0,1}e_1 - m_1 g_1}{e_1 + g_1} - D\right)x_1 - I_{1,2}x_2 f_{1,2}(x_1), \tag{20c}$$

$$\frac{de_2}{dt} = v_{1,2}\left(\frac{g_1 + \rho_{1,2}e_1}{g_1 + \rho_{1,2}} f_{1,2}(x_1) - e_2\right), \tag{20d}$$

$$\frac{dx_2}{dt} = \left(\frac{v_{1,2}e_2 - m_2 g_2}{e_2 + g_2} - D\right)x_2 - I_{2,3}x_3 f_{2,3}(x_2), \tag{20e}$$

$$\frac{de_3}{dt} = v_{2,3}\left(\frac{g_2 + \rho_{2,2}e_2}{g_2 + \rho_{2,3}} f_{2,3}(x_2) - e_3\right), \tag{20f}$$

$$\frac{dx_3}{dt} = \left(\frac{v_{2,3}e_3 - m_3 g_3}{e_3 + g_3} - D\right)x_3. \tag{20g}$$

The first term on the right-hand sides of Eqs. (20c), (20e) and (20g) is due to growth and dilution. The last right-hand side term of Eqs. (20a), (20c), (20e) and (20g) is due to predation by the next level in the food chain. Uptake of food x_{i-1} by trophic level i is via the scaled Holling type II functional response $f_{i-1,i}$ Eq. (13): a hyperbolic function with values between 0 and 1, which is more realistic than a linear functional response. The uptake rate is bound to a maximum, $I_{i-1,i}$. Eqs. (20b), (20d) and (20f) are constitutive relations for the scaled energy density e_i, which is scaled to the maximum energy density, see Table 1. The expression $g_{i-1}\ _{i-1,i}/(g_{i-1} + \ _{i-1,i})$ relates to assimilation of the structural part, and for the reserves we have $\ _{i-1,i-1,i}/(g_{i-1} + \ _{i-1,i})$, so that their sum equals $\ _{i-1,i}$. The growth rate of population i reaches its theoretical maximum value $v_{i-1,i}/g_i = \mu_{i-1,i}$, when $f_{i-1,i}$ and e_i both approach 1, $m_i = 0$, $g_i = \infty$ and $v_{i-1,i} = \infty$.

4.1. Products and non-limiting nutrients

When the system (20) is solved one can calculate the rate of formation of products and the consumption of non-limiting nutrients together with waste-heat production. These rates are proportional to the fluxes for assimilation, maintenance and growth, see (4). Let q_i denote the mass densities in the chemostat of the products and non-limiting nutrients formed and consumed by trophic level i.

The products and non-limiting nutrients leave the reactor via the outlet with the dilution rate D.

Then the dynamics of the sum of the products and non-limiting nutrients is for trophic level $i = 1, 2, 3$,

$$\frac{dq_i}{dt} = \sum_{c\in\{C,H,O,N,\ldots\}} J_{ci} - Dq_i, \tag{21}$$

where J_{ci}, $c\in\{C, H, O, N, \ldots\}$ is given in Eq. (19). This equation can also be derived from system 20 directly by considering the changes of the total biomass of the populations $x_i + z_i = (1 + e_i = (_ig_i))x_i$, $i = 1, 2, 3$

$$\frac{dx_0}{dt} = (x_r - x_0)D - I_{0,1}f_{0,1}x_1, \tag{22a}$$

$$\frac{d(1+e_1\gamma_1 g_1)x_1}{dt} = \left(\frac{v_{0,1}}{\gamma_1 g_1}f_{0,1} - \frac{m_1}{\gamma_1} - \left(\frac{1}{\gamma_1} - 1\right)\left(\frac{v_{0,1}e_1 - m_1 g_1}{e_1 + g_1}\right)\right)x_1 - Dx_1\left(1 + \frac{e_1}{\gamma_1 g_1}\right) - I_{1,2}f_{1,2}x_2\left(1 + \frac{e_1}{\gamma_1 g_1}\right), \tag{22b}$$

$$\frac{d(1+e_2\gamma_2 g_2)x_2}{dt} = \left(\frac{v_{1,2}}{\gamma_2 g_2}\frac{g_1 + \rho e_1}{g_1 + \rho}f_{1,2} - \frac{m_2}{\gamma_2} - \left(\frac{1}{\gamma_2} - 1\right)\left(\frac{v_{1,2}e_2 - m_2 g_2}{e_2 + g_2}\right)\right)x_2 - Dx_2\left(1 + \frac{e_2}{\gamma_2 g_2}\right) - I_{2,3}f_{2,3}x_3\left(1 + \frac{e_2}{\gamma_2 g_2}\right), \tag{22c}$$

$$\frac{d(1+e_3\gamma_3 g_3)x_3}{dt} = \left(\frac{v_{2,3}}{\gamma_3 g_3}\frac{g_2 + \rho e_2}{g_2 + \rho}f_{2,3} - \frac{m_3}{\gamma_3} - \left(\frac{1}{\gamma_3} - 1\right)\left(\frac{v_{2,3}e_3 - m_3 g_3}{e_3 + g_3}\right)\right)x_3 - Dx_3\left(1 + \frac{e_3}{\gamma_3 g_3}\right), \tag{22d}$$

where the dynamics of e_i is again given by Eqs. (20b), (20d) and (20f) for $i = 1, 2, 3$, respectively. The density of product and non-limiting nutrient masses for trophic level i, q_i, is now obtained as that part of the ingested material that does not become part of to the two biomass components of the population

$$\frac{dq_1}{dt} = \left(I_{0,1} - \frac{v_{0,1}}{\gamma_1 g_1}\right)f_{0,1}x_1 + \left(\frac{m_1}{\gamma_1} + \left(\frac{1}{\gamma_1} - 1\right)\left(\frac{v_{0,1}e_1 - m_1 g_1}{e_1 + g_1}\right)\right)x_1 - Dq_1, \tag{23a}$$

$$\frac{dq_i}{dt} = \left(I_{i-1,i}\left(1 + \frac{e_{i-1}}{g_{i-1}}\right) - \frac{v_{i-1,i}}{\gamma_i g_i}\frac{g_{i-1} + \rho e_{i-1}}{g_{i-1} + \rho}\right)f_{i-1,i}x_i + \left(\frac{m_i}{\gamma_i} + \left(\frac{1}{\gamma_i} - 1\right)\left(\frac{v_{i-1,i}e_i - m_i g_i}{e_i + g_i}\right)\right)x_i - Dq_i. \tag{23b}$$

As is expected, the expression for the product formation for each level is the same as those given in Eq. (19).

4.2. A special case

In Kooi and Hanegraaf (2001), we proved that the solution of system (20) is bounded by considering an overall biomass conservation of all biomasses: nutrients, structural, reserves and products, expressed in C-moles, defined as

$$K(t) = x_0(t) + \textstyle\sum_{i=1}^{3}(x_i(t) + z_i(t)). \tag{24}$$

For this total mass it can be shown that the following equation holds

$$\frac{dK}{dt} = -(K(t) - x_r)D. \tag{25}$$

In the long term we have $K = x_r$. It can be shown that for $i = 0, 1, 2, 3$, $x_i(t) \geq 0$ and for $i = 1, 2, 3$, $z_i(t) \geq 0$. Consequently $q_i(t) \geq 0$, $i =$

Table 2
Parameter values used for the calculation of bifurcation diagrams with system (20)

Parameter	unit	Values		
		$i=1$	$i=2$	$i=3$
$K_{i-1,i}$	mg dm^{-3}	8	9	10
$I_{i-1,i}$	h^{-1}	1.25	0.33	0.25
m_i	h^{-1}	0.025	0.01	0.0075
g_i	–	80.0	1.0	0.504
$v_{i-1,i}$	h^{-1}	40.0	0.2	0.0756

As described in Kooi et al. (1998), the parameter values are derived from the values estimated by Nisbet et al. (1983) with a bacterium–ciliate model.

Table 3
List of bifurcations curves and bifurcations points

Symbol	Description
Bifurcation curves	
$TC_{e,i}$	Transcritical: boundary between non-invadability and invadability by population i via an equilibrium
$TC_{c,i}$	Transcritical: boundary between non-invadability and invadability by population i via a limit cycle
H_i	Hopf: boundary, in an area of i-trophic positive coexistence between stable equilibrium and stable limit cycle

Subscripts: e, equilibrium; c, limit cycle; i, number of trophic level.

1, 2, 3 yields that the total biomass $x_0(t) + \Sigma_{i=1}^{3}(x_i(t) + z_i(t))$ is bounded. However, in order to show that $q_i(t) \geq 0$, the terms associated with the growth in 23 give problems because they can become negative when growth is reversed. Therefore, we considered in Kooi and Hanegraaf (2001), the special case $\gamma_i = 1$ where these terms are zero. This is allowed since γ_i does not occur in the state 20. Thus $q_i(t) \geq 0$, $i = 1, 2, 3$ and as a result the total mass is bounded also with $\gamma_i < 1$.

In Kooi and Hanegraaf (2001) we showed that in this special case when $\gamma = 1$ the reserves and the structure must have the same chemical composition, and that the chemical reaction equation for growth Eq. (7) is,

$$\tilde{h}_E C_1 H_{n_{HE}} O_{n_{OE}} N_{n_{NE}} \overset{\text{reserves, } E}{\rightarrow} \tilde{h}_E C_1 H_{n_{HE}} O_{n_{OE}} N_{n_{NE}} \overset{\text{structural mass, } V}{} \quad (26)$$

with no product nor heat formation.

The special case deserves our attention as it is consistent with the utilization of structural biomass for maintenance purposes at times when the density of the reserves is too small to fulfil the need for maintenance. Therefore, we reconsidered the long-term dynamics of the food chain and studied the boundaries of the regions of the bifurcation diagrams where the maintenance requirements can be fulfilled by the utilization of reserves only. The growth rates denoted by $\mathscr{M}_{i-1,i}(e_i(t))$ are defined by,

$$\mathscr{M}_{i-1,i}(e_i(t)) \overset{\text{def}}{=} \frac{v_{i-1,i} e_i(t) - m_i g_i}{e_i(t) + g_i}, \quad i = 1, 2, 3. \quad (27)$$

Thus the individual grows when $\mathscr{M}_{i-1,i}(e_i(t)) > 0$ and shrinks when $\mathscr{M}_{i-1,i}(e_i(t)) < 0$. Growth ceases when $\mathscr{M}_{i-1,i}(e_i(t)) = 0$, that is

$$e_i(t) = \frac{m_i g_i}{v_{i-1,i}}, \quad i = 1 \text{ or } 2 \text{ or } 3. \quad (28)$$

In equilibrium we have $\mathscr{M}_{2,3} = D > 0$ for the top-predator population. For the prey and predator population $\mathscr{M}_{i-1,i} > D > 0$, $i = 1, 2$ because of the extra removal term due to predation.

5. Bifurcation analysis

Bifurcation analysis (Guckenheimer and Holmes, 1985; Kuznetsov, 1998) provides information about the long-term dynamic behaviour of non-linear dynamic systems. Long-term co-existence of trophic levels is qualified as, for instance, equilibrium, limit cycles or chaos, in a bifurcation diagram. The structural stability of the dynamic systems is studied with respect to so-called bifurcation parameters. In the case of the continuous culture the bifurcation parameters are the dilution rate D and the concentration of nutrient in the reservoir x_r, which are parameters that can be controlled in an experiment. When the solution of a system of state equations changes its qualitative character or trophic levels disappear completely under slight adjustment of a bifurcation parameter, the system is structurally unstable. The point in the

parameter space where this happens is called a bifurcation point. Bifurcation curves mark the borders between qualitatively different regions. Bifurcation curves and points relevant for a food chain in continuous culture are listed in Table 3. We used software packages AUTO (Doedel et al., 1997) and LOCBIF, Content (Kuznetsov and Levitin, 1997) and in-house programs to calculate bifurcations curves.

The parameter values are those for a microbial food chain and are the same as used in Kooi et al. (1999), see Table 2, thus allowing comparison with food chains where the reserves are not utilized (Kooi et al., 1999) or not present (Boer et al., 1998). Due to the parameter values for the prey the full system 20 happens to be stiff. In order to circumvent numerical problems and time-consuming computations when calculating the bifurcation diagram, the dynamics of the scaled reserves biomass density of the prey is assumed to be quasi-static; $e_1(t) = f_{0,1}(x_0(t))$. In this way the seven dimensional system 20 is reduced to six dimensions.

5.1. Consumption of the structural component only

Before we study the dynamics of the tri-trophic food chain we describe the results for the simpler bi-trophic food chain briefly and we refer to Kooi and Hanegraaf (2001) for an extensive discussion. In Fig. 3, we show the two-parameter bifurcation diagram for the bi-trophic nutrient–prey–predator food chain in the chemostat for $\rho_{i-1,i} = 0$. There are three biologically important regions separated by a transcritical bifurcation curve denoted by $TC_{e,2}$ and a Hopf bifurcation curve denoted by H_2. Let D be fixed and we will increase x_r. For very low nutrient inflow both prey and predator are washed-out. Crossing the transcritical bifurcation curve $TC_{e,1}$ the nutrient supply is sufficient to support the prey only. Increasing x_r, at the transcritical bifurcation point $TC_{e,2}$ both populations remain in the reactor and there is a stable equilibrium. Increasing the nutrient supply further this equilibrium becomes unstable at the Hopf bifurcation point H_2 and a stable limit cycle originates. This is associated

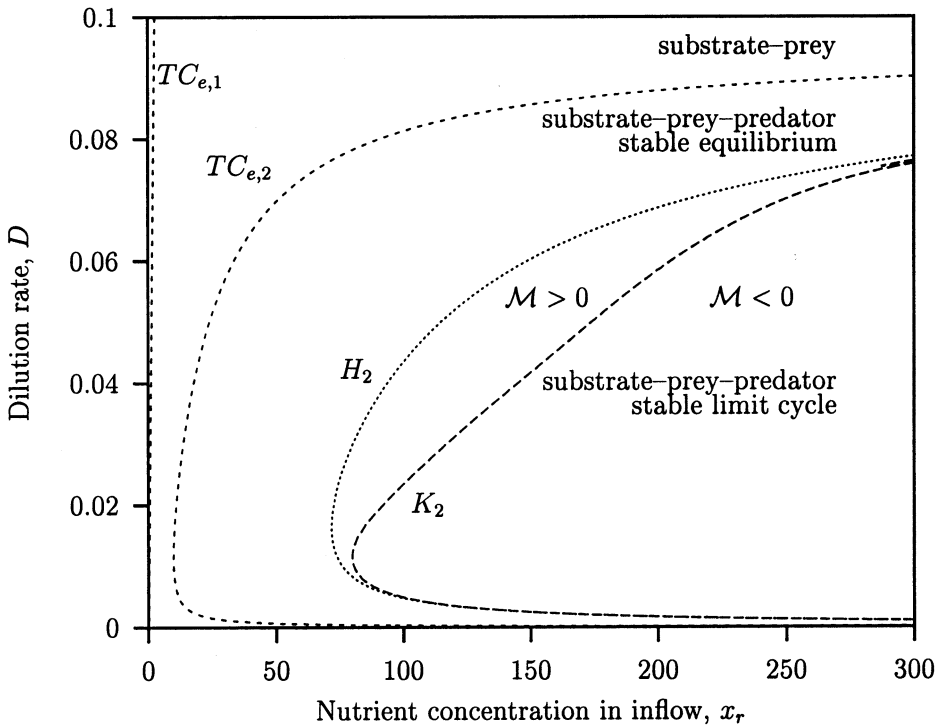

Fig. 3. Bifurcation diagram for DEB model with two trophic levels: system (20) with $\rho_{i-1,i} = 0$. Values assigned to physiological parameters are listed in Table 2. The curves $TC_{e,1}$ and $TC_{e,2}$ are transcritical bifurcation curves and H_2 marks a Hopf bifurcation curve. To the right of curve K_2 the reserve density is not sufficient to pay the costs of maintenance, see Eq. (28).

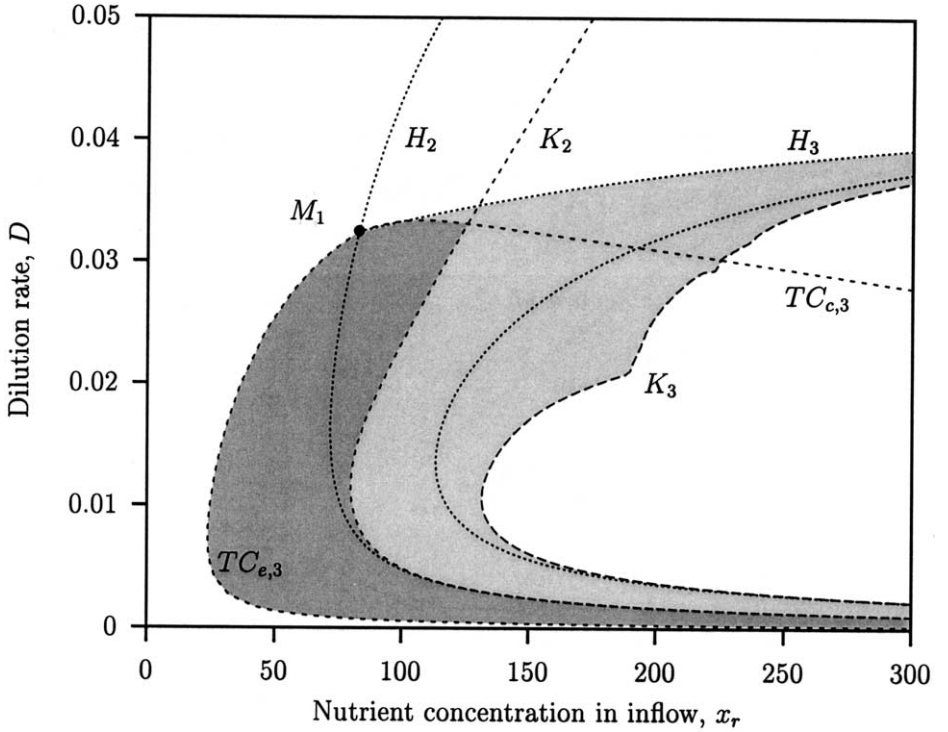

Fig. 4. Regions within a tri-trophic bifurcation diagram. The bifurcation curves are for system 20 with three trophic levels, calculated with $\rho_{i-1,i}=0$ for trophic levels $i=2$, 3, and the parameter values in Table 2. Symbols are listed in Table 3. In the gray region, below $TC_{c,3}$ tri-trophic coexistence is possible by invasion. Between $TC_{e,3}$ and H_3: stable equilibrium; between H_3 and K_3: stable limit cycles; right of K_3 maintenance cannot be paid by reserves Eq. (28). Above the gray region, that is above $TC_{c,3}$, the dynamic behaviour depends on the initial conditions or is unstable. Curves H_2 are K_2 are for the bi-trophic chain also shown in Fig. 3.

with the 'paradox of enrichment' (Rosenzweig, 1971). What happens when the curve K_2 is crossed will be explained below for the more general tri-trophic food chain case.

In Fig. 4, the bifurcation diagram of the tri-trophic food chain of which the dynamics is described by system (20) is shown. The point M_1 is an 'organizing center'. In this point a Hopf bifurcation curve H_2 of the bi-trophic food chain intersects with a transcritical bifurcation $TC_{e,3}$. A transcritical bifurcation curve for limit cycles $TC_{c,3}$ and a Hopf bifurcation curve H_3 originate in M_1.

The transcritical bifurcation curve $TC_{c,3}$ divides the region where the bi-trophic food chain cycles (on the right-hand side of H_2) into two regions. Below the transcritical bifurcation curve $TC_{c,3}$ the top-predator can invade the cycling bi-trophic food chain. In these regions invasion results in stable equilibrium to the left of H_3, and to stable limit cycles at the right of H_3. Above the curve $TC_{c,3}$ invasion by introduction of a small amount of top-predator is impossible, but there can be multiple attractors where dynamic behaviour depends on the initial conditions. When a sufficient amount of top-predator is present initially, stable equilibrium or stable limit cycles or even complex dynamics behaviour such as chaos can be attained, but the top-predator can also go extinct. We refer to Kooi et al. (1998) where the bifurcation curves for the $\rho_{i-1,i}=0$ case were already discussed in detail. Similar (x_r, D) bifurcation diagrams are found and discussed for tri-trophic chains modelled with maintenance and a Holling type II functional response in Boer et al. (1998), Kooi et al. (1998), Hanegraaf et al. (2000), Gragnani et al. (1998).

5.2. Extinction due to starvation

A new situation occurs for the $\rho_{i-1,i}=0$ case when the reserves density becomes too small to

pay for maintenance in a large region of the bifurcation diagram where the long-term dynamics is non-stationary. This phenomenon will also be found for the bifurcation diagrams where the reserves of the prey are assimilated next to structure, that is $\rho_{i-1,i} > 0$ discussed in the next section.

On curves K_i, $i = 2, 3$, the minimum value of $e_i(t)$, $i = 1, 2, 3$, is given by condition Eq. (28). To the left of the curves K_i, in Fig. 4 the structure of top-predator does not shrink. The curves K_i are calculated by testing for condition Eq. (28) during one stable limit cycle, that is for $0 \leq t \leq T_0$ where T_0 is the period of the cycle. As we examine long-term behaviour, these tests were performed after the populations ran through a large number of cycles so that the transient dynamics died out. The free parameter values for curves K_i, $i = 2, 3$, were calculated by testing the solution of 20 for condition Eq. (28) at increasing values of the reservoir density x_r, starting on the H_i curves. Not only the top-predator, but all trophic levels where tested for shrinkage of structure to fulfil maintenance demands. The calculations reveal that to the right of curves K_3 the reserve density of the top-predator is too low to meet the maintenance requirements. The curve K_3 is irregular in regions where the oscillatory dynamics of the food chain is complex, close to chaotic behaviour that originates via a cascade of period doubling when D is held constant while x_r is increased.

Observe that the region, where coexistence of the three species is possible, is also on the right-hand side of K_2 in Fig. 4. Thus when the toppredator goes extinct the solution converges to the limit cycle for the bi-trophic food chain but then the growth of the predator ceases and this population goes extinct too and only the prey remains in the reactor. Visa versa, invasion of the top-predator is only feasible not only below $TC_{c,3}$ but also at the left-hand side of K_2 where the bi-trophic food chain exists. This is the dark gray region in Fig. 4. In this region of the bifurcation diagram the ecosystem can develop in a constant environment from only nutrients, via a nutrient–prey, nutrient–prey–predator system to a nutrient–prey–predator–top-predator system, when the prey, predator and top-predator are introduced one after the other in small quantities. In the light gray region of Fig. 4 this type of ecosystem development in a constant environment is impossible. In this region the tri-trophic food chain permanent community can develop via a change of environmental conditions (that is, a change in the parameter values of x_r and D), or by introduction of invaders in sufficiently large quantities.

The curves K_i, $i = 2, 3$ lie to the right and immediately above the Hopf curves H_i, $i = 2, 3$, respectively. It is not surprising that these curves can lie so close to the Hopf curves because the amplitude of the cycles increases quadratically when the bifurcation parameters move away from the Hopf parameter values (Kuznetsov, 1998).

We mention without further discussion that stable limit cycles occur also in a small region close to M_1 above H_3 in Fig. 4 and also here extinction due to starvation is possible depending on the vital parameter values.

5.3. Influence of assimilation of the reserve component

Our main goal is to study the influence of the assimilation of the reserves and structure of the prey on the dynamics of a tri-trophic food chain under various environmental conditions. To this end we compare bifurcation diagrams for different values for the assimilation efficiencies of the structural and the reserve component of the prey, given by the parameters $\rho_{i-1,i}$, $i = 2, 3$. We recall that since for the parameter value $g_1 = 80$, for moderate values of $\rho_{1,2}$, the consequences for the bi-trophic food chain are negligible, for we have in Eq. (20d) $(g_1 + \rho_{1,2}e_1)/(g_1 + \rho_{1,2}) \approx 1$, since $0 \leq e_1 \leq 1$.

In Fig. 5 the long-term behaviour of system (20) is shown for $\rho_{i-1,i} = 1$ for $i = 2, 3$ defined in Eq. (17). We will treat the features that are similar in both diagrams Figs. 4 and 5. The gray regions in Fig. 5 indicate the areas where coexistence for the whole tri-trophic food chain can be attained.

The region in the parameter space where positive coexistence via invasion of the top-predator can occur, is smaller for $\rho_{i-1,i} = 1$ than for $\rho_{i-1,i} = 0$, and calculations showed that this effect is stronger for larger $\rho_{i-1,i}$. When $\rho_{i-1,i}$ increases the point M_1 (the intersection of the curves $TC_{e,3}$ and H_2) moves downwards along the curve H_2. This is explained

as follows. Since we want to compare food chains where the trophic levels have the same theoretical maximum growth rate, $\mu_{i-1,i} = v_{i-1,i}/g_i$ for $i = 1, 2, 3$, we keep $v_{i-1,i}$ constant and different ratios of the assimilation rates are examined by changing $\rho_{i-1,i}$, $i = 2, 3$. When $\rho_{i-1,i} = 0$ only structure is utilized and when the reserves are assimilated with a higher efficiency, $\rho_{i-1,i} > 0$, structure is assimilated less efficiently, that is $(g_{i-1} + {}_{i-1,i}e_{i-1})/(g_{i-1} + \rho_{i-1,i}) < 1$. The scaled reserve biomass density e_i is always smaller than its maximum value of 1. We conclude that when reserves are assimilated next to structure, the total contribution of prey components to the reserve of the predator is smaller than when only structure is assimilated.

6. Discussion

In the present article trophic levels can become extinct at high supply rates of the limiting nutrient, because at some point in a stable limit cycle the density of the reserves can become too small to pay the costs of maintenance Eq. (28). In our model, individuals consist of two components, reserves and structure. When the reserve density is insufficient, the integrity of structure cannot be maintained and the individual dies. The organism dies because its reserves become too lean: maintenance condition Eq. (28) is therefore in essence a starvation condition. Since we assumed all individuals indentical this leads directly to extinction of the population and possibly indirectly to extinction of other populations as well. This type of collapse of the ecosystem due to starvation of populations in the food chain in regions with oscillatory dynamic behaviour, such as period solutions and even chaos, can be commonly found in model systems describing ecosystems, and therefore may explain why attempts to observe chaos in natural population

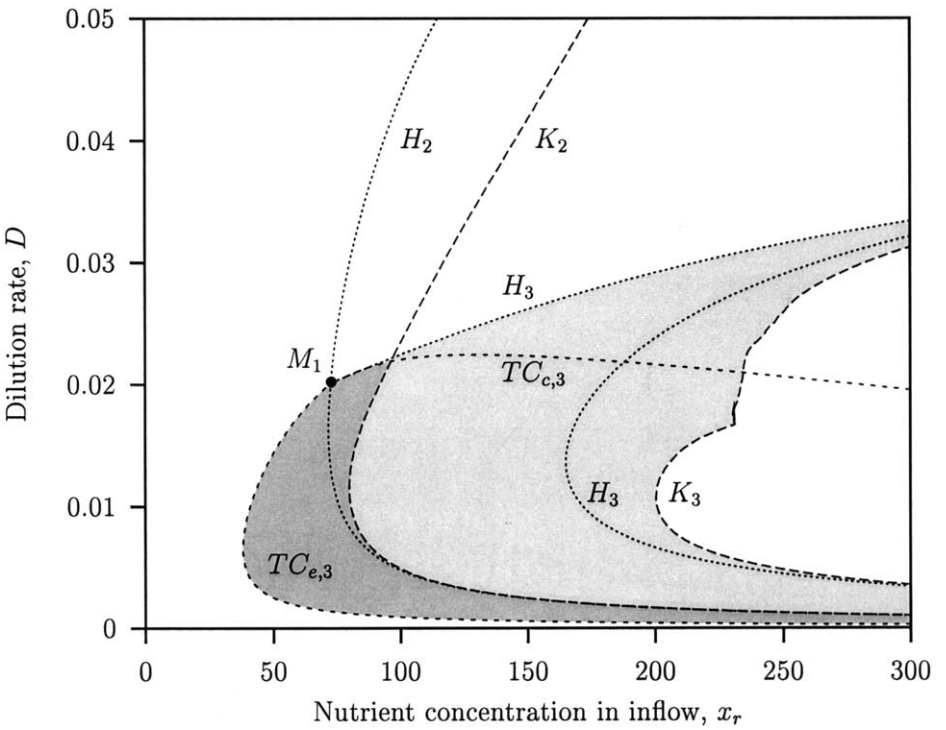

Fig. 5. Bifurcation diagram for system 20 with three trophic levels, calculated with assimilation of both structural and reserve component, $\rho_{i-1,i} = 1$ for trophic levels $i = 2, 3$. Stable positive coexistence for the whole tri-trophic food chain is possible in the gray region. In the dark gray region this is possible via successive invasions of higher trophic levels in a constant environment (constant x_r and D values). In the light gray region coexistence is possible via succession where the environment changes or via successive introduction of a new top-species in large quantities.

have failed. Below we will survey other model choices than dying.

The cause of the effects of enrichment in this article differs from the phenomenon known as 'paradox of enrichment' (Rosenzweig, 1971) which concerns the appearance of oscillations at high food input. These oscillations are sometimes referred to as unstable population dynamics. However, sustainable oscillations in the form of stable limit cycles, are a form of stable population dynamics, just like stable equilibria, see also Vayenas and Pavlou (1999). Also in this article permanent coexistence in sustainable oscillations is not disrupted because of 'unstable' population dynamics, but via a form of starvation.

An important aspect of the paradox of enrichment is that increased supply rates of the limiting nutrient may lead to "[…] extinction due to demographic stochasticity" (Fryxell and Lundberg, 1998; Rosenzweig, 1971; May, 1972; Gilpin, 1972). Experimental observations of this effect of nutrient enrichment have been found in field and laboratory studies (see DeAngelis, 1992, Chapter 5). In the present article we are able to calculate the precise boundaries for extinction (the K-curves) with the starvation condition Eq. (28). This starvation criterion is therefore more tangible than a criterion for extinction via stochastic effects which is caused by too 'small' numbers of prey. A stochastic criterion is in need of an objective definition of 'small' numbers of prey.

In our model, reserves are used for growth (that is, the increase of structure) when the reserve density is more than sufficient for the maintenance demand. When the reserves become too small to pay for maintenance the system of state equations allows reversed growth: structure shrinks to supplement the reserves. Although reversed growth is allowed by the system of state equations for the food chain Eqs. (20), the reverse growth process is unrealistic from a biochemical perspective because it has no overhead costs in the form of heat or product formation. Therefore, we can choose to let individuals die when they cannot pay their maintenance costs, which means that the top-predators do not survive in the large areas to the right of the K_3 lines in Figs. 4 and 5. In the chemostat with time-invariant control parameters (that is, the dilution rate and the concentration of the nutrient in the inflow), death by starvation occurs only for non-stationary long-term dynamics. In Muller and Nisbet (2000) survival of an organism in variable resource environments is studied. In that paper the DEB model (Kooijman, 2000) is used to describe the dynamics of an individual where reproduction is taken into account explicitly. Also in their study, death occurs when the rate at which the reserves are used is insufficient to meet maintenance costs.

An alternative model choice, to make reversed growth feasible, is to define a new parameter for the cost of transformation of structure into reserves in the reverse growth reaction. However, this leads to a switch where at some point reserves are transformed into structure and vice versa. Moreover, many species specific choices are possible; for instance, microorganisms may enter a resting state or invest in spore formation just before the reserves are too small to pay for maintenance. Various other model choices can be made to decide what happens at the point where the reserve density is too small to pay maintenance.

Food chain models become more relevant for the description of real biological communities (food webs) by considering multiple nutrients or multiple prey per trophic level, so that predators can choose prey types or that prey species can compete for limiting nutrients (Vayenas and Pavlou, 1999; Abrams, 1999; Gragnani et al., 1999; Vayenas and Pavlou, 2001). Here we considered a different way to add realism. In this paper the components of a prey can differ in their chemical composition and can be assimilated with different efficiencies, which means that they have a different nutritional value for the predator. Just as the edibility of prey is relevant (Gragnani et al., 1999), it matters for the dynamics of the predator which prey component has the highest nutritional value.

When the assimilation of prey reserves is more efficient than assimilation of prey structure, the Hopf bifurcation curve H_3 and the K_3 curve interfere with the area of stable equilibrium at higher values of Dx_r. In Fig. 5, for $\rho_{i-1,i}=1$ this region starts at much lower values of Dx_r then the stable limit cycles for $\rho_{i-1,i}=0$ in Fig. 4. So, a major effect of reliance of a predator on prey reserves is that the stable limit cycles and the starvation criterion are found at high values of food input.

The bifurcation diagrams show that the presence of reserves in preys and predators affects long-term behaviour of the communities also in other ways. An important effect of consumption of reserves is via the maximum growth rate. The maximum growth rate is reached when e_{i-1} equals one (besides $f_{i-1,i}=1$) and e_{i-1} approaches one in the long term at conditions of high food availability. However, the reserve density never reaches its maximum in continuous culture. So, when all parameters are identical, this effect will cause a lower growth rate than in models without reserves. As the growth rate affects the area of invadability (high growth rate, easy invadability (Kooi et al., 1999)), we fixed the maximum growth rate for each trophic level when we compare different assimilation efficiencies for prey reserves and structure. As a consequence, a higher efficiency of reserve assimilation implies a lower efficiency of assimilation of structure and vice versa. However, we still see the effect of the reserve density in Fig. 5 when the reserves of the prey are consumed by the predator. Because the prey can have varying reserve densities, but the reserves never reach its maximum density, the yield of the predator reserves is smaller when the predator assimilates prey reserves with greater efficiency and prey structure with smaller efficiency.

We adopted the view that the processes of assimilation, maintenance and growth should be regarded as biochemical reaction equations (Hanegraaf, 1997; Kooijman et al., 1999; Kooijman, 2000; Kooi and Hanegraaf, 2001; Hanegraaf and Muller, 2001), as in Roels (1983), Nielsen and Villadsen (1994). The description of the compounds via their molecular formulas facilitates a biogeochemical model formulation where interaction is via products and minerals, or when nutrient recycling is modelled. Working with enthalpy instead of free energy, as in Kooijman et al. (1999), Kooi and Hanegraaf (2001), makes the link with experimental data easier since enthalpy of the different compounds involved can be measured directly using bomb calorimetry (Kondepudi and Prigogine, 1998). When experimental data for nutrient consumption and product formation are available in addition to growth data of the population, better parameter estimations can be obtained.

Most important is that the biochemical reaction equations provide information that is simply not present in state equations. The efficiency of growth process denoted by γ does not appear in the state equations (20) but is present in system (22) and also in the expressions (23) for the rate of product formation. Biochemical reaction equations characterize compounds by their molecular formulas and internal energies and enable the construction of elemental balances and thermodynamic balances including mass and energy exchanges with the environment. It is this information which prohibits reversed growth, which in turn has such a profound effect on the bifurcation diagrams.

7. Conclusions

Simple models are of use for many applications, and a simple set of state equations can be suited to illustrate a theoretical point. The minimal version of the dynamic energy budget model used here includes reserves, next to structure. We revised the population interaction terms to take into account that the predator population consumes prey individuals that consists of two components with different nutritial value. The well-tried method of the biochemical representation of model equations make some model choices apparent because it can provide information that is not necessarily present in a system of state equations. In the exemplary case described in this article, the biochemical perspective, together with the individual based modelling approach, focused our attention on the consequences of reversed growth.

It is concluded that the decision to disallow shrinking of structure to pay the costs of maintenance when reserves are less than needed, affects a major area of coexistence in the bifurcation diagrams. It is in these areas that entire trophic levels can go extinct. The starvation criterion proposed here is more tangible than a criterion for extinction of 'small' amounts of biomass via stochastic effects. We agree with Muller and Nisbet (2000) that there is a need for better mechanistic models of mortality due to starvation.

If the nutritial value of the reserves increases, coexistence occurs at decreasing dilution rates because the reserve density is always lower than its

maximum. This is the price an organism has to pay for surviving relatively short periods of food shortage. When the reserves of the prey are of increasing importance as a source of food for the predator, the region of stable equilibrium extents to higher values of food input rate.

Our work on the tri-trophic food chain illustrates that reaction equations and mass–energy coupling can be applied in biogeochemical models where nutrient recycling is important.

Acknowledgements

This research is supported by grant number 805.39.751 of The Netherlands Technology Foundation (STW), and is coordinated by the Council of Earth and Life Sciences (ALW).

References

Abrams, P.A., 1999. The adaptive dynamics of consumer choice. The American Naturalist 153 (1), 83–97.

Boer, M.P., Kooi, B.W., Kooijman, S.A.L.M., 1998. Food chain dynamics in the chemostat. Mathematical Biosciences 150 (1), 43–62.

DeAngelis, D.L., 1992. Dynamics of Nutrient Cycling and Food Webs. Number 9 in Population and Community Biology Series. Chapman & Hall, London.

Doedel, E.J., Champneys, A.R., Fairgrieve, T.F., Kuznetsov, Y.A., Sandstede, B., Wang, X., 1997. Auto 97: continuation and bifurcation software for ordinary differential equations. Technical Report, Concordia University, Montreal, Canada.

Droop, M.R., 1983. 25 years of algal growth kinetics; a personal view. Bot. Mar. 26, 99–112.

Fryxell, J.M., Lundberg, P., 1998. Individual Behaviour and Community Dynamics. Population and Community Biology Series. Chapman & Hall, London.

Gilpin, M.E., 1972. Enriched predator–prey systems: theoretical stability. Science 177, 902–904.

Gragnani, A., De Feo, O., Rinaldi, S., 1998. Food chains in the chemostat: relationships between mean yield and complex dynamics. Bulletin of Mathematical Biology 60, 703–719.

Gragnani, A., Scheffer, M., Rinaldi, S., 1999. Top-down control of cyanobacteria: a theoretical analysis. The American Naturalist 153 (1), 59–72.

Guckenheimer, J., Holmes, P., 1985. Nonlinear Oscillations, Dynamical Systems and Bifurcations of Vector Fields. In: Applied Mathematical Sciences, vol. 42, 2nd ed. Springer-Verlag, New York.

Hanegraaf, P.P.F., 1997. Mass and energy fluxes in microorganisms according to the energy budget theory for filaments. Ph.D. thesis, Vrije Universiteit Amsterdam, Amsterdam, The Netherlands.

Hanegraaf, P.P.F., Kooi, B.W., Kooijman, S.A.L.M., 2000. The role of intracellular components in food chain dynamics. Comptes Rendus de l'Academie Des Science Series III—Sciences de la vie-life 323, 99–111.

Hanegraaf, P.P.F., Muller, E.B., 2001. The dynamics of the macromolecular composition of biomass. Journal of Theoretical Biology 212 (2), 237–251.

Jørgensen, S.E. (Ed.), 2001. Thermodynamics and Ecological Modelling. Lewis Publishers, Boca Raton, FL.

Kondepudi, D., Prigogine, I., 1998. Modern Thermodynamics. Wiley, New York.

Kooi, B.W., Boer, M.P., Kooijman, S.A.L.M., 1998. Consequences of population models on the dynamics of food chains. Mathematical Biosciences 153 (2), 99–124.

Kooi, B.W., Boer, M.P., Kooijman, S.A.L.M., 1999. Resistance of a food chain to invasion by a top predator. Mathematical Biosciences 157, 217–236.

Kooi, B.W., Hanegraaf, P.P.F., 2001. Bi-trophic food chain dynamics with multiple component populations. Bulletin of Mathematical Biology 63 (2), 271–299.

Kooijman, S.A.L.M., 2000. Dynamic Energy and Mass Budgets in Biological Systems. Cambridge University Press, Cambridge.

Kooijman, S.A.L.M., Kooi, B.W., Hallam, T.G., 1999. The application of mass and energy conservation laws in physiologically structured population models of heterotrophic organisms. Journal of Theoretical Biology 197 (3), 371–392.

Kuznetsov, Y.A., 1998. Elements of Applied Bifurcation Theory. In: Applied Mathematical Sciences, vol. 112, 2nd ed. Springer-Verlag, New York.

Kuznetsov, Y.A., Levitin, V.V., 1997. CONTENT: Integrated environment for the analysis of dynamical systems. Centrum voor Wiskunde en Informatica (CWI), 1.5 ed. Kruislaan 413, 1098 SJ Amsterdam, The Netherlands.

Lange, K., Oyarzun, F., 1992. The attractiveness of the Droop equations. Mathematical Biosciences 111, 261–278.

Loladze, I., Kuang, Y., Elser, J.J., 2001. Stoichiometry in producer-grazer systems: linking energy flow with element cycling. Bulletin of Mathematical Biology 62, 1137–1162.

May, R.M., 1972. Limit cycles in predator–prey communities. Science 177, 900–902.

Muller, E.B., Nisbet, R.M., 2000. Survival and production in variable resource environments. Bulletin of Mathematical Biology 62, 1163–1189.

Nielsen, J.H., Villadsen, J., 1994. Bioreaction Engineering Principles. Plenum Press, New York.

Nielsen, S.N., 2000. Thermodynamics of an ecosystem interpreted as a hierarchy of embedded systems. Ecological Modelling 135, 279–289.

Nielsen, S.N., Ulanowicz, T.E., 2000. On the consistency between thermodynamical and network approaches to ecosystems. Ecological Modelling 132, 23–31.

Nisbet, R.M., Cunningham, A., Gurney, W.S.C., 1983. Endogenous metabolism and the stability of microbial prey–predator systems. Biotechnology and Bioengineering 25, 301–306.

Odum, E.P., 1996. Ecology A Bridge Between Science and Society. Sinauer Associates Inc., Sunderland, MA.

Polis, G.A., Winemiller, K.O. (Eds.), 1996. Food Webs. Chapman & Hall, New York.

Roels, J.A., 1983. Energy and Kinetics in Biotechnology. Elsevier Biomedical Press, Amsterdam.

Rosenzweig, M.L., 1971. Paradox of enrichment: destabilization of exploitation ecosystems in ecological time. Science 171, 385–387.

Vayenas, D.V., Pavlou, S., 1999. Coexistence of three microbial populations competing for three complementary nutrients in a chemostat. Mathematical Biosciences 161, 1–13.

Vayenas, D.V., Pavlou, S., 2001. Chaotic dynamics of a microbial system of coupled food chains. Ecological Modelling 136 (2–3), 285–295.